para *tert*-butyl). ^{1}H-decoupled ^{13}C NMR ($CDCl_3$) showed resonances at the following chemical shifts in ppm from internal standard tetramethylsilane: 31.52, 34.64, 34.96, 37.43, 121.40, 148.11, 158.25, and 159.68. The highest *m/e* fragment observed was the tri-*tert*-butylphenyl radical cation at *m/e* 245 (44.9%) and 246 (9.1%).

X-ray quality crystals of III were grown by dissolving the compound in a 10:1 pentane/octane mixture. Slow evaporation of this solution afforded colorless hexagonal plates of III. The crystals were protected from light since III rapidly darkened on exposure to sunlight. The crystal selected for X-ray diffraction measured 0.05 × 0.15 × 0.15 mm.

X-ray Structure Analysis. The crystal was mounted on a goniometer head by using silicone grease. The diffractometer utilized was designed and constructed locally. A Picker four-circle goniostat equipped with a Furnas monochromator (HOG crystal) and Picker X-ray generator (Mo Kα radiation, λ = 0.710 69 Å) is interfaced to a TI980 minicomputer, with Slo-Syn stepping motors to drive the angles. Centering is accomplished by using automated top/bottom–left/right slit assemblies. The minicomputer is interfaced by low-speed data lines to a CYBER172-CDC6600 multi-mainframe system where all computations are performed. In the present case the crystal system, space group, and approximate unit-cell dimensions were determined during a preliminary investigation. The quality of the crystal was shown to be adequate on the basis of ω scans which showed the peak width at half-height to be ca. 0.20°. The unit-cell dimensions were subsequently refined from the Bragg angles of 23 reflections [$C_{36}H_{58}Hg$, M_r = 691.44, monoclinic, space group $P2_1/c$; at −155 °C, a = 19.830 (15) Å, b = 10.309 (7) Å, c = 18.919 (13) Å, β = 120.69 (6)°, Z = 4, V = 3326 Å^3, D_{calcd} = 1.381 g cm^{-3}, linear absorption coefficient = 46.45 cm^{-1}].

Intensity data were collected by using the 2θ scan technique (4° < 2θ < 55°; scan rate = 2.0° min^{-1}; single background time at extremes of scan = 15 s). The scan width was 2.0° plus dispersion; 6418 reflections were recorded at −155°. Due to the size of the crystal and the linear absorption coefficient, an absorption correction was made which ranged from 0.359 to 0.638.

The structure was solved by using a combination of direct methods and Patterson techniques. The structure was refined by the full-matrix least-squares method using 5259 reflections for which $F > 2.33\sigma(F)$. The atomic scattering factors were taken from the tabulations of Cromer and Waber;[21a] anomalous dispersion corrections were by Cromer.[21b] The standard deviations of the observed structure factors $\sigma(F_o)$ were based on counting statistics and an "ignorance factor", p, of 0.02.[22] The Hg and *tert*-butyl C atoms were refined with anisotropic thermal parameters; the H and phenyl C atoms were refined with isotropic thermal parameters. The final residuals were $R(F)$ = 0.037 and $R_w(F)$ = 0.043.

Acknowledgment. We wish to thank Dr. David Pensak for many helpful discussions and for carrying out molecular mechanics as well as molecular orbital calculations to probe the origin and nature of these distortions and the M. H. Wrubel Computing Center for computational time.

Registry No. II, 74063-08-4; III, 74063-09-5.

Supplementary Material Available: Tables of the anisotropic thermal parameters, the hydrogen distances, the hydrogen bond angles, the torsion angles, the bonded and nonbonded distances, the idealized hydrogen positions, and the bonded and nonbonded contacts as well as the idealized coordinates (60 pages). Ordering information is given on any current masthead page.

(21) "International Tables for X-ray Crystallography"; Kynoch Press: Birmingham, England, 1974; Vol. IV: (a) Table 2.2B; (b) Table 2.3.1.
(22) Corfield, B. W. R.; Doedens, R. J.; Ibers, J. A. *Inorg. Chem.* **1967**, *6*, 197.

Contribution No. 3505 from the Department of Chemistry and Molecular Structure Center, Indiana University, Bloomington, Indiana 47405

A Donor Semibridge? Molecular Structures of Dicyclopentadienyldivanadium Tetracarbonyl Triphenylphosphine and Dicyclopentadienyldivanadium Pentacarbonyl

J. C. HUFFMAN, L. N. LEWIS, and K. G. CAULTON*

Received January 25, 1980

The compound $Cp_2V_2(CO)_4PPh_3$, Ib, has been synthesized by photochemical substitution on the parent carbonyl, $Cp_2V_2(CO)_5$, Ia. The crystal and molecular structure of the phosphine derivative has been determined at −130 °C. The space group is $P\bar{1}$ with cell constants a = 8.225 (2) Å, b = 16.806 (4) Å, c = 10.193 (3) Å, α = 102.13 (2)°, β = 101.91 (2)°, and γ = 83.84 (1)°. Full-matrix least-squares refinement of 3989 reflections resulted in $R(F)$ = 0.088. For comparison, the crystal structure of $Cp_2V_2(CO)_5$ has been redetermined at −150 °C. The metal–metal bond length in Ib, 2.466 (1) Å, is essentially identical with that in the parent carbonyl and is indicative of a multiple bond. The overall molecular structure of Ib is similar to that of the parent carbonyl. A detailed comparison of the bond lengths and angles at the semibridging carbonyls in Ib with those in the parent carbonyl was made in an attempt to evaluate whether or not the semibridging interaction in both compounds involves a donation of electron density from the CO bond to a neighboring electron-deficient vanadium. This attempt is precluded by asymmetry at the carbonyl semibridges in Ia. The origin of this asymmetry is traced to end-to-end nonbonded contacts in these sterically crowded dimers.

Introduction

The compound $Cp_2V_2(CO)_5$, Ia, is noteworthy in several respects.[1] It is not the obvious extension of the homologous series $Cp_2Ni_2(CO)_2$, $Cp_2Co_2(CO)_3$, $Cp_2Fe_2(CO)_4$, $Cp_2Re_2(CO)_5$, $Cp_2Cr_2(CO)_6$. Although Ia has a formula related to $Cp_2Re_2(CO)_5$, II, the structures differ markedly.[2] The rhenium dimer has only one bridging carbonyl, which is symmetrically disposed with respect to the metal atoms. The vanadium dimer has no symmetric CO bridges;[3] it may be roughly described as consisting of $CpV(1)(CO)_3$ and $CpV(2)(CO)_2$ units, held together by a short (2.46 Å) metal–metal bond *and* two asymmetrically bridging CO groups. The asymmetric bridges are disposed in a noncompensating fashion,[4] and both of the carbonyl ligands involved are strongly

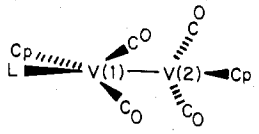

Ia, L = CO
b, L = PPh_3

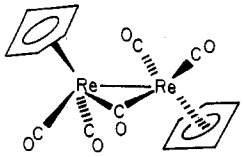

II

(1) Fischer, E. O.; Schneider, R. J. *Chem. Ber.* **1970**, *103*, 3684.
(2) Foust, A. S.; Hoyano, J. K.; Graham, W. A. G *J. Organomet. Chem.* **1971**, *32*, C65.
(3) Cotton, F. A.; Frenz, B. A.; Kruczynski, L. *J. Am. Chem. Soc.* **1973**, *95*, 951; *J. Organomet. Chem.* **1978**, *160*, 93.

0020-1669/80/1319-2755$01.00/0

bound to the $CpV(CO)_3$ fragment. The two carbonyls are nearly but not precisely equivalent to each other; we shall return to this point.

Noncompensated semibridging carbonyls[5] appear to exist in order to moderate charge imbalance. Past examples have included only situations where the semibridge is created to accept electron density from a neighboring electron-rich metal center. Examples[4] include $Fe_2(CO)_7(bpy)$, $Fe_2(CO)_6(C_4R_4)$ ("ferroles"), and $FeCo(CO)_8^-$. The V–V σ bond in $Cp_2V_2(CO)_5$ has been described[4] as coordinate covalent (from V(1) to V(2)). This donor bonding is claimed to make V(2) formally electron rich, a condition which is then alleviated by electron donation *from* V(2) to the two CO semibridges (III). For simplicity, this will be called an acceptor semibridge.

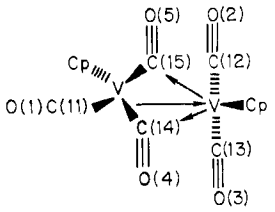

III

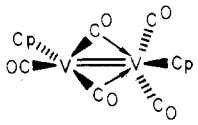

IV

We found this description somewhat paradoxical since an alternative formulation, built around a covalent V–V double bond, has V(1) saturated and V(2) electron deficient (16 electron configuration)! Post hoc reasoning with this model would suggest that the semibridging occurs so as to donate electron density from the π orbitals of the two semibridging ligands to the unsaturated vanadium (a "donor semibridge"; see IV). Since V(2) possesses a 16-electron configuration prior to semibridging, the proposed donor semibridge ligands in Ia individually donate less than a full two electrons. The prototype donor semibridge, which does involve donation of a full two electrons from the CO π system, is found in $Mn_2(CO)_5(dpm)_2$.[6,7]

We describe here the results of our attempt to distinguish between bonding models III and IV.

Experimental Section

Synthesis of Ib. $Cp_2V_2(CO)_2$[1] (0.15 g, 0.4 mmol) and PPh_3 (0.1 g, 0.4 mmol) were combined in a Pyrex glass tube in 10 mL of tetrahydrofuran. This solution was maintained below 25 °C while it was photolyzed with a medium-pressure Hg arc lamp for 30 min. The solution was purged with N_2 during irradiation. Following irradiation, $Cp_2V_2(CO)_4PPh_3$ was precipitated by slow addition of hexanes. Crystals suitable for the diffraction study were grown by slow addition of hexanes to a solution of Ib in benzene. The compound had spectroscopic properties consistent with those previously reported.[1] The mass spectrum showed the ions $Cp_2V_2(PPh_3)(CO)_n^+$, $n = 1$–3, as well as smaller fragments; no parent ion was detected at 70 eV and a sample temperature of 220 °C.

Crystallography. General Data. The diffractometer used in this study consisted of a Picker goniostat interfaced to a TI980B minicomputer with 56K words of 16 bit memory. The angle drives of the goniostat were interfaced by using Slo-Syn stepping motors and translator driver boards. The computer is programmed to operate on an interrupt basis by using a precision internal clock, and the scan speeds are controlled by the pulse rate delivered to the translator driver boards. Each pulse will drive the corresponding goniostat angle 0.005°, and virtually any angular rate can be chosen. A "filter attenuator wheel", mounted on the detector arm, is positioned such that up to 20 apertures or attenuators can be automatically located in the diffraction beam path. Apertures are provided for automatic top/bottom–left/right centering of reflections, and these are utilized for both goniostat and crystal alignment. Standard "NIM-bin" electronics are used for pulse shaping and energy discrimination, and the computer-controlled timer and scaler were constructed locally.

Reflection data are collected in a normal θ–2θ scan mode with backgrounds at each extreme of the scan. A buffer is provided so that up to 4800 reflection data can be stored in the computer memory. In addition to the normal teletype for control and hard-copy output, the TI980B is interfaced to a CDC6600 computer via a 9600 baud link through a minicomputer network, and to a CYBER172, via 300 baud data lines. Interactive terminals with graphics capability are available in the Molecular Structure Center to communicate with the CYBER172, and a high speed card reader and line printer are available to the CDC6600 through a "remote job entry" millicomputer. The CYBER172 and CDC6600 operate in a multimainframe configuration by using the KRONOS operating system.

Low-Temperature Facilities. A liquid-nitrogen boil-off cooling system is used to maintain all samples at −140 to −180 °C. The system used consists of two 30-L storage Dewars to supply the dry nitrogen gas for the cold stream and concentric warm stream and a third 30-L recooling Dewar through which the cooling gas is passed. The recooling Dewar consists of a coil (2-m length) of copper tubing which is joined to an evacuated and silvered glass delivery tube. The delivery tube is designed to supply the cold nitrogen in a fixed position from the bottom of the χ circle. The exit nozzle is carefully streamlined to ensure a laminar flow, and details of its construction are available.[8] Thermocouples and heating wires located in the exit nozzle monitor and control the temperature. Short-term temperature fluctuation is typically ±0.2 °C with long-term stability of ±3 °C. The entire cooling system, including supply and recooling Dewars, consumes approximately 10–20 L of liquid nitrogen/day and will operate for a period of several weeks with no substantial frosting problems. Locally constructed goniometers which minimize frosting and eliminate collision problems on the goniostat are used. Crystals are mounted on glass fibers by using a silicon grease, which remains amorphous and becomes rigid at the normal operating temperature of the system.

Software. All programs can be run either in an interactive mode or as "batch" jobs. The computer network used in the Indiana University Molecular Structure Center allows data to be rapidly processed while data collection continues. It is thus possible to collect redundant data and quickly test whether any "equivalent" data disagree. The indices of such reflections can be transmitted back to the laboratory minicomputer system for recollection. It is often possible to obtain a trial structure in a matter of hours in order to determine if it is well-ordered and significant enough to warrant a more extensive data set. The interactive process permits rapid application of direct methods procedures. If the data do not yield a structure, a more extensive set can be collected.

Data are reduced by using the equations $I = C - 0.5(t_c/t_b)(B_1 + B_2)$ and $\sigma(I) = [C + 0.25(t_c/t_b)^2(B_1 + B_2) + (pI)^2]^{1/2}$, where C is the total integrated peak count obtained in scan time t_c, B_1 and B_2 are the background counts obtained in time t_b, and p is the "ignorance factor".[9]

The function minimized in the least-squares program is $\sum w|F_o - F_c|^2$ where $w = 1/\sigma(F_o)$, and residuals are defined as $R(F) = \sum||F_o| - |F_c||/\sum|F_o|$ and $R_w(F) = (\sum w||F_o| - |F_c||^2/\sum wF_o^2)^{1/2}$.

$(C_5H_5)_2V_2(CO)_4P(C_6H_5)_3$. A well-formed parallelepiped was used for all characterization and data collection. All data were collected at −130 ± 4 °C. The crystal was characterized by indexing a set of

(4) Cotton, F. A. *Prog. Inorg. Chem.* **1976**, *21*, 1.
(5) The original categorization of unsymmetrical bridging carbonyl ligands subdivided these into "...two basically different sorts..."[4]: *semibridges*, characterized by both molecular and local carbonyl asymmetry, and *compensating sets* of unsymmetrical bridges. The latter category includes only cases where local asymmetry occurs in a compensatory fashion so as to maintain equivalence of the metal atoms (i.e., retention of a rotational axis of symmetry). We will argue that semibridges are not limited to donation of a maximum of two electrons, as are the CO's in a compensating unsymmetrical set. Because of this functional inequivalence, we will adhere strictly to the original definition of semibridging as a category which excludes compensating sets. Note, however, that current usage has tended to obscure this original distinction.
(6) Colton, R.; Commons, C. J. *Aust. J. Chem.* **1975**, *28*, 1673.
(7) Caulton, K. G.; Adair, P. *J. Organomet. Chem.* **1976**, *114*, C11. The anion $HFe_4(CO)_{13}^-$ also contains a 4-electron donor CO but one in which the unique ligand interacts with all four metal centers: Manassero, M.; Sansoni, M.; Longoni, G. *J. Chem. Soc., Chem. Commun.* **1976**, 919.
(8) (a) Huffman, J. C. Ph.D. Thesis, Indiana University. (b) Rudman, R. A. "Low Temperature X-Ray Diffraction"; Plenum Press: New York, 1976.
(9) Corfield, P. W. R.; Doedens, R. J. *Inorg. Chem.* **1967**, *6*, 197.

Table I. Crystal Data for $(C_5H_5)_2V_2(CO)_5$ (Ia) and $(C_5H_5)_2V_2(CO)_4P(C_6H_5)_3$ (Ib)

	Ia	Ib
mol formula	$C_{15}H_{10}O_5V_2$	$C_{32}H_{25}O_4PV_2$
color	green	green
cryst dimens, mm	0.21 × 0.15 × 0.24	0.15 × 0.20 × 0.23
space group	$P2_1/n$	$P\bar{1}$
cell dimens		
a, Å	8.376 (8)[a]	8.225 (2)[b]
b, Å	15.547 (18)	16.806 (4)
c, Å	11.183 (11)	10.193 (3)
α, deg	(90)	102.13 (2)
β, deg	91.78 (9)	101.91 (2)
γ, deg	(90)	83.84 (1)
molecules/cell	4	2
cell vol, Å^3	1455.6	1344.9
D, g/cm^3	1.744	1.498
wavelength, Å	0.710 69	0.710 69
mol wt	382.2	606.4
linear abs coeff, cm^{-1}	12.6	7.66
no. of unique intensities collected	2549	5575
no. with $F > 0.0$	2420	4091
no. with $F > \sigma(F)$	2402	3989
no. with $F > 2.33\ \sigma(F)$	2370	3082
final residuals		
$R(F)$	0.056	0.088
$R_w(F)$	0.085	0.057
goodness-of-fit for last cycle	1.34	1.05
max Δ/σ for last cycle	0.04	0.02

[a] At −150 °C; 17 reflections. [b] At −130 °C; 17 reflections.

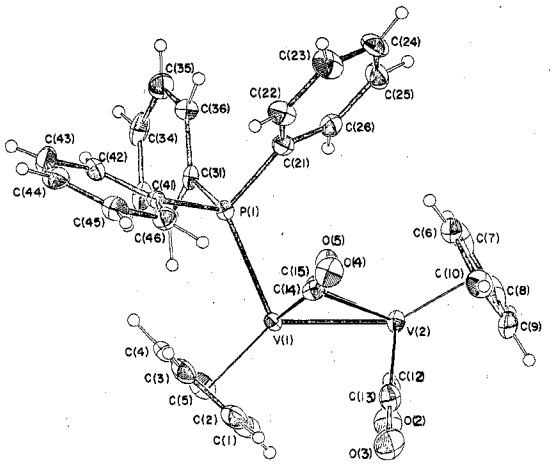

Figure 1. View of $Cp_2V_2(CO)_4(PPh_3)$ perpendicular to the PV(1)V(2) plane. Anisotropic thermal ellipsoids are drawn at the 50% probability level. Hydrogen atoms are portrayed at 0.5 Å^2.

reflections located in a hemisphere of reciprocal space directly on the goniostat. No extinctions or symmetry was observed, and subsequent statistics and solution of the structure indicated the space group $P\bar{1}$. Crystal data and other parameters of the data collection appear in Table I. The source–monochromator–sample and sample–receiving aperature distances were 23.5 and 21.5 cm, respectively. The receiving aperature dimensions were 2.5 mm wide by 3.5 mm high.

A complete sphere of data was collected for the region $4° \leq 2\theta \leq 55°$ and corrected for Lorentz and polarization terms. The data were collected by using a conventional θ–2θ scan technique with a scan rate of 3.0°/min over a range of 2.1° plus a dispersion correction to account for the $K\alpha_1$ and $K\alpha_2$ split. Ten-second background counts were recorded at each extreme of the scan. Three reflections were chosen as standards and monitored after every 100 measurements, and an examination of the intensities of these reflections indicated no systematic trends in the data. The structure was solved and refined during collection of the redundant data, and the 100 reflections with the largest discrepancies between I_{obsd} and I_{calcd} as well as 35 reflections whose difference between the two equivalent measurements differed by more than 2.3 times the average σ (on the basis of counting statistics) were recollected and used in the final averaging.

Table II. Positional[a] and Thermal[b] Parameters for $(C_5H_5)_2V_2(CO)_4P(C_6H_5)_3$

atom	10^4x	10^4y	10^4z	$10B_{iso}$, Å^2
V(1)	5477 (1)	2322 (1)	5701 (1)	11
V(2)	6818 (1)	3481 (1)	7313 (1)	14
P(1)	6283 (2)	2081 (1)	3437 (1)	11
C(1)	4411 (8)	1678 (4)	7030 (7)	28
C(2)	3091 (8)	2102 (4)	6305 (7)	27
C(3)	2944 (7)	1765 (4)	4921 (7)	22
C(4)	4186 (7)	1135 (3)	4777 (6)	18
C(5)	5097 (8)	1074 (4)	5084 (7)	24
C(6)	7902 (8)	4412 (3)	6505 (7)	22
C(7)	9222 (7)	3983 (4)	7183 (8)	28
C(8)	9132 (10)	4119 (4)	8544 (8)	32
C(9)	7712 (9)	4651 (4)	8742 (7)	31
C(10)	6945 (8)	4827 (3)	7455 (6)	23
C(13)	4788 (7)	3696 (3)	8001 (6)	19
C(12)	7371 (6)	2779 (3)	8640 (6)	17
C(15)	7859 (7)	2173 (3)	6225 (5)	13
C(14)	4743 (6)	3377 (3)	5260 (5)	16
O(3)	3597 (6)	3850 (3)	8459 (5)	33
O(2)	7693 (5)	2359 (2)	9418 (4)	27
O(5)	9273 (4)	1948 (2)	6406 (4)	20
O(4)	4097 (5)	3960 (2)	4854 (4)	23
C(21)	7255 (6)	2926 (3)	3108 (5)	16
C(22)	6431 (8)	3443 (8)	2240 (6)	21
C(23)	7195 (8)	4085 (4)	2037 (7)	28
C(24)	8815 (9)	4216 (4)	2676 (7)	31
C(25)	9670 (8)	3707 (4)	3541 (7)	26
C(26)	8894 (7)	3061 (3)	3749 (6)	19
C(31)	7807 (6)	1227 (3)	3015 (5)	14
C(32)	8011 (7)	566 (3)	3663 (5)	16
C(33)	9136 (7)	−85 (3)	3346 (6)	18
C(34)	10134 (7)	−63 (4)	2406 (6)	22
C(35)	9934 (7)	596 (4)	1765 (6)	22
C(36)	8797 (7)	1233 (3)	2059 (6)	18
C(41)	4532 (6)	1905 (3)	1998 (5)	12
C(42)	4590 (6)	1252 (3)	886 (5)	16
C(43)	3246 (7)	1175 (4)	−198 (6)	22
C(44)	1884 (7)	1727 (4)	−231 (6)	22
C(45)	1810 (7)	2359 (4)	871 (6)	20
C(46)	3129 (7)	2447 (3)	1965 (6)	18
H(40)	4798 (72)	1679 (35)	7877 (60)	33 (14)
H(41)	2517 (79)	2523 (39)	6724 (66)	41 (16)
H(42)	2297 (68)	1933 (33)	4221 (56)	24 (13)
H(43)	4509 (71)	806 (35)	4012 (60)	28 (13)
H(44)	5979 (68)	718 (33)	6204 (57)	24 (13)
H(45)	7665 (53)	4405 (26)	5660 (45)	2 (9)
H(46)	9946 (71)	3641 (34)	6901 (59)	28 (14)
H(47)	9797 (87)	3945 (42)	9212 (72)	50 (18)
H(48)	7368 (74)	4848 (36)	9492 (61)	31 (14)
H(49)	6152 (61)	5184 (30)	7280 (51)	12 (11)
H(50)	5523 (54)	828 (26)	887 (44)	0 (9)
H(51)	3333 (64)	759 (33)	−754 (55)	10 (11)
H(52)	1036 (74)	1662 (35)	−1007 (61)	24 (13)
H(53)	843 (68)	2794 (33)	908 (55)	17 (11)
H(54)	3017 (72)	2853 (36)	2731 (63)	25 (13)
H(55)	5395 (65)	3404 (30)	1872 (51)	8 (11)
H(56)	6441 (72)	4446 (35)	1355 (59)	24 (13)
H(57)	9289 (76)	4602 (38)	2495 (63)	26 (14)
H(58)	10831 (71)	3757 (33)	3948 (56)	19 (12)
H(59)	9498 (68)	2634 (33)	4340 (57)	19 (12)
H(60)	7330 (58)	585 (28)	4301 (50)	5 (10)
H(61)	9215 (56)	−510 (29)	3760 (48)	4 (10)
H(62)	10812 (62)	−498 (31)	2124 (51)	8 (10)
H(63)	10558 (75)	609 (36)	1223 (63)	26 (15)
H(64)	8622 (67)	1671 (34)	1547 (57)	21 (12)

[a] Numbers in parentheses in this and all following tables refer to the esd of the least significant digit. [b] The isotropic thermal parameter listed for those atoms refined anisotropically is the isotropic equivalent.

The structure was solved by direct methods (LSAM) and Fourier techniques. Where possible, the atom labeling chosen was identical with that in $Cp_2V_2(CO)_5$.[3] Full-matrix refinement using isotropic thermal parameters for hydrogens and anisotropic thermal parameters for all other atoms rapidly converged, with final residuals of $R(F) = 0.088$ and $R_w(F) = 0.057$. There is no evidence for disorder of

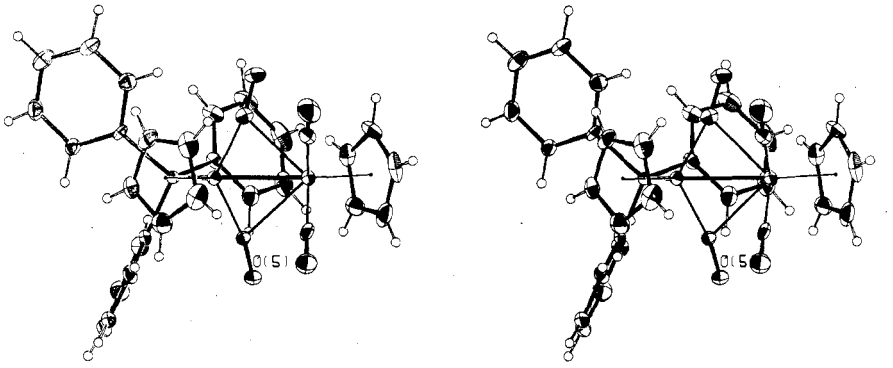

Figure 2. Stereoscopic view of $Cp_2V_2(CO)_4(PPh_3)$ along the edge of the PV(1)V(2) plane.

Table III. Interatomic Distances (Å) in $Cp_2V_2(CO)_4PPh_3$ (Ib) and $Cp_2V_2(CO)_5$ (Ia)

atoms		distance		
		Ib	Ia (25 °C)	Ia (−150 °C)
V(1)	V(2)	2.466 (1)	2.462 (2)	2.459 (3)
V(1)	P(1)	2.472 (2)		
V(1)	C(11)		1.967 (11)	1.972 (4)
C(11)	O(1)		1.144 (10)	1.130 (5)
V(1)	C(14)	1.925 (5)	1.947 (11)	1.941 (4)
V(1)	C(15)	1.925 (5)	1.925 (11)	1.940 (5)
V(1)	C(1)	2.253 (6)		2.242 (5)
V(1)	C(2)	2.264 (6)		2.242 (5)
V(1)	C(3)	2.295 (5)	2.219 (12)[a]	2.267 (5)
V(1)	C(4)	2.291 (5)		2.267 (5)
V(1)	C(5)	2.278 (6)		2.257 (5)
V(2)	C(12)	1.932 (5)	1.911 (12)	1.931 (4)
V(2)	C(13)	1.912 (6)	1.922 (11)	1.912 (5)
V(2)	C(14)	2.400 (5)	2.440 (10)	2.448 (5)
V(2)	C(15)	2.400 (5)	2.402 (10)	2.387 (4)
V(2)	C(6)	2.250 (6)		2.283 (4)
V(2)	C(7)	2.272 (6)		2.260 (4)
V(2)	C(8)	2.289 (6)	2.259 (10)[a]	2.251 (5)
V(2)	C(9)	2.279 (6)		2.255 (5)
V(2)	C(10)	2.247 (6)		2.296 (4)
P(1)	C(21)	1.823 (5)		
P(1)	C(31)	1.842 (5)		
P(1)	C(41)	1.832 (5)		
O(2)	C(12)	1.142 (6)	1.164 (11)	1.156 (5)
O(3)	C(13)	1.152 (6)	1.144 (10)	1.146 (5)
O(4)	C(14)	1.175 (6)	1.161 (11)	1.160 (5)
O(5)	C(15)	1.174 (6)	1.155 (11)	1.155 (5)
C(1)	C(2)	1.389 (9)		1.386 (7)
C(1)	C(5)	1.403 (9)		1.361 (8)
C(2)	C(3)	1.390 (9)	1.31 (3)[a]	1.364 (7)
C(3)	C(4)	1.398 (8)		1.384 (9)
C(4)	C(5)	1.404 (8)		1.416 (10)
	av	1.399 (6)	av[b]	1.382 (22)
C(6)	C(7)	1.381 (8)		1.413 (6)
C(6)	C(10)	1.399 (8)		1.385 (7)
C(7)	C(8)	1.373 (10)	1.39 (1)[a]	1.414 (6)
C(8)	C(9)	1.416 (10)		1.398 (7)
C(9)	C(10)	1.409 (9)		1.415 (7)
	av	1.396 (18)	av[b]	1.405 (13)

[a] Only an average value is reported here, due to uncertainties arising from disorder in Ia at 25 °C. [b] Esd's on average values are calculated by using the scatter formula $\sigma(\text{av}) = [\Sigma(d_i - \bar{d})^2/(N-1)]^{1/2}$, where d_i is one of N individual values and $\bar{d}$ is their average.

cyclopentadienyl carbons (cf. ref 3).

Two views of the molecule are shown in Figures 1 and 2. The final refined parameters are given in Table II; bond lengths and angles are given in Tables III and IV. Table V displays distances of atoms from several least-squares planes. Tables of observed and calculated structure factor amplitudes and further structural parameters are available.

The cyclopentadienyl rings are rigorously planar (maximum deviation of carbon from the least-squares plane is 0.3σ). The refined

Table IV. Intermolecular Angles (Deg) in Compounds Ia and Ib

atoms			angle	
			Ib	Ia (−150 °C)
V(2)	V(1)	P(1) or C(11)	112.9 (1)	111.9 (1)
V(2)	V(1)	C(14)	64.9 (2)	66.4 (1)
V(2)	V(1)	C(15)	64.9 (1)	64.5 (1)
P(1) or C(11)	V(1)	C(14)	81.9 (2)	81.7 (2)
P(1) or C(11)	V(1)	C(15)	79.8 (2)	77.4 (2)
C(14)	V(1)	C(15)	113.1 (2)	113.0 (2)
V(1)	V(2)	C(12)	87.3 (2)	87.7 (1)
V(1)	V(2)	C(13)	86.4 (2)	83.0 (1)
V(1)	V(2)	C(14)	46.6 (1)	46.6 (1)
V(1)	V(2)	C(15)	46.6 (1)	47.2 (1)
C(12)	V(2)	C(13)	82.8 (2)	81.9 (2)
C(12)	V(2)	C(14)	130.2 (2)	131.1 (2)
C(12)	V(2)	C(15)	71.3 (2)	71.1 (2)
C(13)	V(2)	C(14)	77.5 (2)	77.0 (2)
C(13)	V(2)	C(15)	125.6 (2)	122.5 (2)
C(14)	V(2)	C(15)	84.0 (2)	84.0 (2)
V(1)	P(1)	C(21)	114.7 (2)	
V(1)	P(1)	C(31)	118.5 (2)	
V(1)	P(1)	C(41)	114.0 (2)	
C(21)	P(1)	C(31)	100.9 (2)	
C(21)	P(1)	C(41)	103.3 (2)	
C(31)	P(1)	C(41)	103.5 (2)	
V(2)	C(12)	O(2)	179.5 (5)	179.0 (4)
V(2)	C(13)	O(3)	177.1 (5)	176.4 (3)
V(1)	C(14)	O(4)	169.7 (4)	169.4 (3)
V(1)	C(15)	O(5)	168.1 (4)	167.7 (4)
V(2)	C(14)	O(4)	121.5 (4)	123.6 (3)
V(2)	C(15)	O(5)	123.3 (4)	123.7 (3)
C(2)	C(1)	C(5)	108.0 (6)	107.6 (5)
C(1)	C(2)	C(3)	108.5 (6)	108.8 (4)
C(2)	C(3)	C(4)	107.9 (5)	108.8 (5)
C(3)	C(4)	C(5)	108.3 (5)	106.1 (4)
C(1)	C(5)	C(4)	107.4 (6)	108.7 (5)
C(7)	C(6)	C(10)	108.3 (6)	109.0 (4)
C(6)	C(7)	C(8)	109.1 (6)	107.0 (4)
C(7)	C(8)	C(9)	108.2 (6)	108.2 (4)
C(8)	C(9)	C(10)	106.8 (6)	108.1 (4)
C(6)	C(10)	C(9)	107.6 (6)	107.8 (4)
M(1)	V(1)	P(1) or C(11)	112.9	111.8
M(1)	V(1)	C(14)	122.8	121.3
M(1)	V(1)	C(15)	123.7	125.6
M(1)	V(1)	V(2)	134.1	136.3
M(2)	V(2)	C(12)	114.6	113.5
M(2)	V(2)	C(13)	115.2	114.4
M(2)	V(2)	C(14)	115.2	115.4
M(2)	V(2)	C(15)	119.0	122.8
M(2)	V(2)	V(1)	150.1	153.6
V(1)	C(11)	O(1)		178.1 (3)

hydrogen positions lie within 1σ of the C_5 planes, showing no consistent trend toward or away from the metal. Internal ring angles scatter by less than 2σ. The C–C distances within the Cp rings deviate by less than 1.5σ from the average of 1.397 Å. In spite of this high

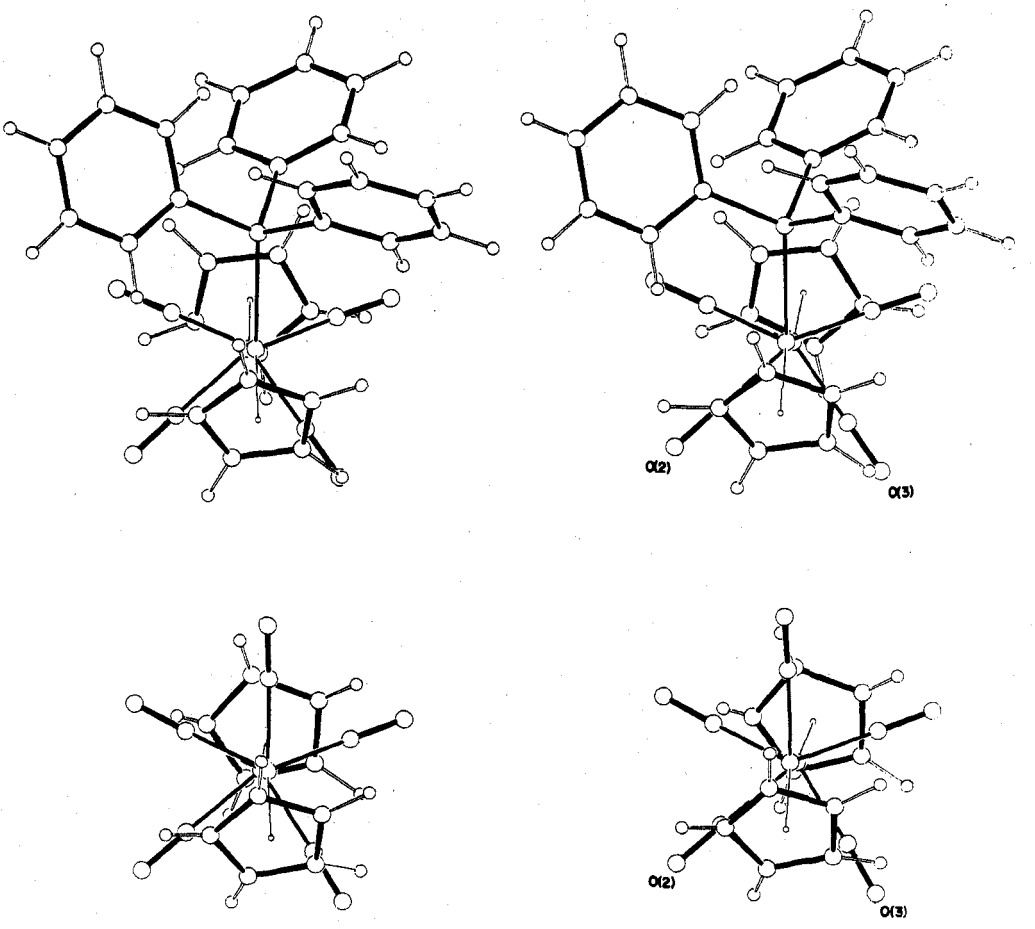

Figure 3. Stereoviews of compounds Ia (lower) and Ib (upper) viewed down the metal–metal bond. V(1) is forward.

Table V. Distances of Atoms from Least-Squares Planes (Å) in $Cp_2V_2(CO)_4PPh_3$ (Ib) and $Cp_2V_2(CO)_5$ (Ia) [Atoms Defining Plane: V(1)/V(2)/P(1) or C(11)]

	dist from plane			dist from plane	
atoms	Ib	Ia (−150 °C)	atoms	Ib	Ia (−150 °C)
M(1)	0.018	0.028	O(4)	−2.70	−2.73
M(2)	−0.108	−0.223	O(5)	2.63	2.54
O(2)	2.27	2.37	C(14)	−1.62	−1.67
O(3)	−1.76	−1.55	C(15)	1.59	1.56
C(12)	1.43	1.49	O(1)		0.036
C(13)	−1.10	−0.99			

internal symmetry, there is a systematic asymmetry in the V–C distances: the three ring carbons which are generally "cis" to the V–V bond (C(6)C(7)C(10) and C(1)C(2)C(5)) exhibit shorter V–C distances. The variations in V–C (2.25–2.29 Å) are as large as 7σ and consistently place the central carbon of the three-carbon unit closer to the metal atom. The proton NMR spectrum of $Cp_2V_2(CO)_4(PPh_3)$ (two Cp chemical shifts) indicates that this intra-ring inequivalence has only a short lifetime. Carbon–hydrogen separations average 0.87 Å for the two cyclopentadienyl rings, ranging from 0.84 (5)–0.93 (6) Å. Atom V(1) lies 1.94 Å from the ring least-squares plane; the analogous separation for V(2) is 1.93 Å.

The shortest nonbonded intramolecular contacts not involving hydrogen in $Cp_2V_2(CO)_4(PPh_3)$ are C(12)–C(13), at 2.54 Å, and C(12)–C(15), at 2.55 Å. Intramolecular contacts of the type cyclopentadienyl carbon/carbonyl, phenyl carbon/carbonyl and cyclopentadienyl carbon/phenyl carbon exceed 2.84, 3.04, and 3.40 Å, respectively. Excluding hydrogens, there are nine intermolecular contacts below 3.5 Å, the shortest (3.20 Å) of which involves O(4) and C(2).

The parameters internal to triphenylphosphine are normal. The C–C distances within the phenyl rings are not equal but show a systematic tendency for longer bonds to the carbon bound to phosphorus (1.394 (7) Å) than elsewhere (1.383 (7) Å).

$(C_5H_5)_2V_2(CO)_5$. The crystal employed was grown from benzene/hexane. Crystal data and parameters of the data collection are given in Table I. The space group is the same as that of the crystal used by Cotton;[3] unit-cell parameters differ significantly at +25 and −150 °C. Intensities were collected in the range $4° \leq 2\theta \leq 55°$. Refinement was initiated by using the coordinates determined at 25 °C. All atoms refined normally with the exception of those of the cyclopentadienyl ring attached to V(1). Thermal parameters of carbons in this ring suggest disorder at 25 °C.[3] The several atoms of that ring which did not converge were located by a difference Fourier synthesis, phased on those atoms which refined satisfactorily. The room-temperature parameters of this ring are inappropriate for refining our data since *only* this ring is rotated ~36° from the conformation reported by Cotton.[3] The resulting conformation closely resembles that in $Cp_2V_2(CO)_4(Ph_3)$. This provides a rather striking example of the benefits of collecting X-ray data at low temperature. In other respects, however, the crystallographic results at +25 and −150 °C are remarkably similar. Bond lengths from the low-temperature data set are within 2σ (25 °C) of those reported by Cotton, with the major improvement (in addition to the Cp ordering) being σ values reduced by 50–70%. Hydrogen atoms were located and refined isotropically by using our data.

The atom-labeling scheme is identical with that employed earlier[3] for Ia; this, in turn, is identical with Figure 1, except for replacement of P(1) by C(11)O(1). Views of both Ia and Ib down the metal–metal vector are shown in Figure 3. Bond lengths and angles are shown in Tables III and IV. Table V contains distances of atoms from several least-squares planes. Tables of fractional coordinates, anisotropic thermal parameters, and structure factor amplitudes are available as supplementary material.

The cyclopentadienyl rings are planar (carbons deviate from the least-squares plane by less than 1σ), and the refined hydrogens deviate by at most 0.2 Å (3σ) to both sides of the carbon planes. Internal

Table VI. Carbonyl Stretching Frequencies (cm^{-1}) in THF

$Cp_2V_2(CO)_5$	1990	1944	1890	1858	1817
$\Delta\nu$	(–)	(14)	(20)	(38)	(47)
$Cp_2V_2(CO)_4PPh_3$		1930	1870	1820	1770
assignt	C(11)O(1)	C(12)O(2), C(13)O(3)		C(14)O(4), C(15)O(5)	

ring angles scatter by less than 4σ, and C–C distances deviate by less than 3σ from their average. Carbon–hydrogen separations average 0.92, ranging from 0.61 (6) to 1.09 (6) Å. Each metal atom is 1.92 Å from its associated ring least-squares plane. Ring planes make angles of 89.4° (V(1)) and 88.6° (V(2)) with lines from the metal to ring centers of gravity. Distances from metals to the associated ring carbons display an inequality also present in Ib; deviations are 0.025 Å (4σ) for V(1) and 0.045 Å (8σ) for V(2).

Results and Discussion

Synthesis and Structure. Photosubstitution of CO in $Cp_2V_2(CO)_5$ by PPh_3 produces $Cp_2V_2(CO)_4PPh_3$, Ib. This reaction produces the same isomer as that produced earlier[1] in a thermal reaction (2 days at 25 °C). We have never observed NMR or infrared evidence for any other isomer.

The infrared spectrum of $Cp_2V_2(CO)_4(PPh_3)$ in the 1600–2200-cm^{-1} region, when compared to that of $Cp_2V_2(CO)_5$, may be interpreted in terms of substitution of the unique CO in the pentacarbonyl by PPh_3. This argument[10] may be developed by using Table VI. Since all vibrations of each molecule are infrared active, the disappearance of one band on substitution is expected and observed. The frequencies in Table VI have been correlated to minimize $\Delta\nu$, the frequency change on substitution. With this correlation accepted, it is the highest carbonyl frequency of $Cp_2V_2(CO)_5$ which is lost. Since C(11) has the longest terminal VC bond in $Cp_2V_2(CO)_5$, we concluded that this, the unique carbonyl, would have the highest intraligand vibrational frequency. This model ignores the reality of vibrational coupling. Nevertheless, it can be extended to derive a reasonable corollary result. The values of $\Delta\nu$ for two bands drop less than 20 cm^{-1} on phosphine substitution, while the reduction of the other two frequencies is 2–3 times as large. Since C(12)O(2) and C(13)C(3) are terminal and distal to the site of substitution, they should be both higher in frequency and less sensitive to phosphine substitution than C(14)C(4) and C(15)O(5) (semibridging and proximal to added phosphine). These crude vibrational assignments are summarized in Table VI.

Molecular Structures. Our attempt to distinguish experimentally between bonding models III and IV will be based on the response of donor and acceptor semibridges to phosphine substitution. It is therefore appropriate to list the predicted phosphine-induced structural changes by using the donor semibridge and acceptor semibridge models. The guiding principle here is that anything which tends to increase electron density at the "altruistic" carbonyl will enhance the donor capacity of a donor semibridge. Replacement of CO by phosphine at V(1) is one such alteration. Conversely, this same alteration will diminish the acceptor capacity of an acceptor semibridge. Thus we anticipate that the V(2)–C (semibridge) distance will shorten or lengthen on phosphine substitution at V(1) if the semibridges donate or accept, respectively.

The structure of $Cp_2V_2(CO)_4PPh_3$ found in the crystal is in agreement with that deduced from spectroscopic data. The molecular skeleton (excluding the phenyl rings) approximates mirror symmetry, the idealized mirror plane passing through V(1), V(2), P(1), and M(1)[11] (see Table V; this plane is vertical in Figure 3). Point M(2) lies significantly (0.11 Å) out of this plane with the result that the Cp ring centers are not precisely staggered (Figure 3). This places C(13) and O(3) closer than C(12) and O(2) to the V(1)V(2)P plane. Associated with this distortion is a statistically significant (4σ) inequality in V–CO distances from V(2) to C(12) and C(13). We shall return to this point.

In the course of evaluating the structural results for Ib, it became apparent that the limited accuracy in the previous X-ray study of Ia precluded any firm conclusions. We were particularly troubled by the inequality reported in the longer pair of V–C semibridge distances (Table III) in view of the fact that these distances are identical in Ib. A redetermination of the structure of Ia was therefore carried out at −150 °C in the hope that these features were actually an artifact. It was therefore gratifying to find that the inequality (0.025 Å, 2σ) previously observed in the distances from V(1) to C(14) and C(15) had vanished in our work at −150 °C. These distances in Ia are marginally longer (0.015 Å, 2σ) than in the phosphine derivative Ib. This lengthening is comparable to that in $Cr(CO)_5PPh_3$[12] (0.029 Å) and confirms the increased back-donation from V(1) to the semibridging carbonyls in Ib.

The two terminal carbonyl ligands in $Cp_2V_2(CO)_4(PPh_3)$, those attached to V(2), have V–C distances identical with their counterparts in the pentacarbonyl; this indicates that phosphine substitution has no structural consequence at the unsubstituted metal. The C–O distances for these two ligands in Ib are 4σ shorter than those in the semibridging ligands, consistent with standard back-bonding arguments. The separations of C(12) and C(13) from V(1) (in excess of 3 Å) are nonbonding.

The metal–metal separations in Ia and Ib are essentially identical (they differ by 0.007 Å or 2σ). This insensitivity to phosphine substitution is consistent with previous observations on other multiply bonded dimers. For example, $Re_2Cl_8^{2-}$[13] and $Re_2Cl_6(PEt_3)_2$[14] contain quadruple bonds different in length by 0.006 Å; these compounds contain a covalent (i.e., not dative) multiple bond.

Our low-temperature study confirms that the unique carbonyl in $Cp_2V_2(CO)_5$ is bound to V(1) by an unusually long bond. The associated CO bond is shorter (3σ) than in the carbonyls bound to V(2). While this supports the basic premise of our vibrational assignment, there is no evidence for a correspondingly long V–P bond in $Cp_2V_2(CO)_4PPh_3$; the V–P separation here (2.472 Å) compares to a value of 2.49 Å in $(\eta^3\text{-}C_3H_5)V(CO)_4PPh_3$.[15]

The structural details of the interaction of the two CO semibridges with V(2) constitutes the central result of this study. This interaction involves only carbon; V(2)–O distances in both Ia and Ib exceed 3 Å. Phosphine substitution reduces the V(2)–C(14) distance by 0.048 Å (7σ), but it *lengthens* V(2)–C(15) by 0.013 Å (2σ); the harsh reality of the situation is that the asymmetry reported earlier[3] is real! The inequality of the distances from V(2) to the two semibridge carbons amounts to 0.061 Å, or 9σ, and makes it impossible to establish the character of the semibridge bonding as originally planned. The nature of this distortion from molecular mirror symmetry is evident in Figure 3. This view down the V–V axis shows the angular deformation present in *both* Ia and Ib. This is the most evident in the positions of the terminal carbonyls and to a lesser extent the C_5H_5 ring on V(2). The torsional angle M(1)V(1)V(2)M(2) is 174.3° in Ib and 166.2°, or over 8° smaller, in Ia. The larger angular distortion in $Cp_2V_2(CO)_5$ than in $Cp_2V_2(CO)_4PPh_3$ is also evident in Table V, as well as Figure 3. The planes V(1), V(2), and P(1) or C(11) are potential molecular mirror planes. In Ib, mirror symmetry about V(1) is maintained to within 0.07 Å; this degrades

(10) A similar argument is presented in ref 3.
(11) M(*i*) designates the midpoint of the cyclopentadienyl ring on metal atom V(*i*).

(12) Plastas, H. J.; Stewart, J. M.; Grim, S. O. *Inorg. Chem.* **1973**, *12*, 265.
(13) Cotton, F. A.; Hall, W. T. *Inorg. Chem.* **1977**, *16*, 1867.
(14) Cotton, F. A.; Foxman, B. M. *Inorg. Chem.* **1968**, *7*, 2135.
(15) Schneider, M.; Weiss, E. *J. Organomet. Chem.* **1976**, *121*, 189.

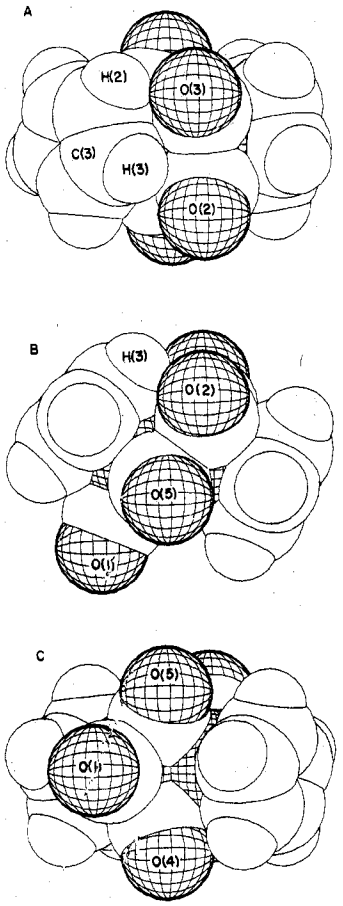

Figure 4. Space-filling models of $Cp_2V_2(CO)_5$ with V(1) at left and V(2) at right (peripheral hatched atoms are oxygen; central hatched atoms are vanadium; hydrogen atoms are positioned by assuming C–H = 1.08 Å): (A) view with terminal carbonyls on V(2) projecting forward; (B) a 90° rotation about the horizontal axis from A; (C) an additional 90° rotation (terminal CO on V(1) projects forward).

somewhat at V(2). In Ia, however, the larger deviations about V(2) induce asymmetry in ligands on V(1). An examination of nonbonded contacts in Ia, using hydrogen positions calculated by assuming a C–H distance of 1.08 Å, reveals the O(3)···H(2) contact to be 2.57 Å (H(2) is attached to C(2)); this contact, between *opposite ends* of the dimer, is less than the sum of the van der Waals radii. This contact and the several contacts between both terminal carbonyls on V(2) and the Cp ring on V(1) are evident in Figure 4.[16] This figure also shows the gear-and-cog nature of the interaction of the C(12)O(2)/C(13)O(3) pair with the Cp ring on V(1); the C(3)–H(3) vector lies in the crevice formed by these two terminal carbonyls. Parts B and C of Figure 4 reveal that the three remaining carbonyls experience no correspondingly short contacts; in particular, Figure 4B makes it clear that there is ample room for bulky $P(C_6H_5)_3$ to replace C(11)O(1). The potential, but unrealized, mirror plane of symmetry lies horizontally in Figure 4A. It is clear that the short intramolecular O(3)···H(2) contact has precisely the directional character to distort the $CpV(2)(CO)_2$ unit as observed and therefore represents the "cause" of the distortion. Of course, if the C(3)–H(3) vector lay in the C(11)V(1)V(2) plane, the end-to-end repulsions would not prevent the C(12)O(2)/C(13)O(3) pair from achieving mirror symmetry. It thus becomes necessary to determine why the ring on V(1) assumes its asymmetric rotational conformation. This can be traced to intermolecular nonbonded repulsions, being 2.37 Å to H(4) from O(4) related by $(1 + x, y, z)$ and 2.40 Å to H(2) from O(5) related by $(x - 0.5, 0.5 - y, z - 0.5)$.[17] Consistent with the lower density of $Cp_2V_2(CO)_4PPh_3$, there are no intermolecular contacts to hydrogens on ring 1 shorter than 2.7 Å. Ring 1 in the phosphine derivative rotates slightly but significantly so that the O(3)···H(2) contact lengthens by 0.1 Å. Distortions at V(2) are correspondingly diminished in Ib, and the longer semibridge distances achieve equality.

In summary, we are able to specify particular nonbonded intermolecular contacts which in turn cause intramolecular distortions. These are felt most strongly by the weakest bonds in the molecule, the longer carbonyl semibridge bonds.

Phosphine substitution has a remarkably small effect on the unusual molecular geometry found in $Cp_2V_2(CO)_5$. This is especially evident in the negligible angular distortion of the vanadium coordination spheres which results on phosphine substitution (Table IV). We conclude that the CO semibridges in both Ia and Ib, regardless of the nature of the interaction, are performing an essential stabilizing role and that there are no isomeric forms of similar free-energy content (cf. $Fe_3(CO)_{12}$[4] and $Cp_3Co_3(CO)_3$[18]). The molecular structure is rigid enough to persist unchanged in different crystalline environments and also, apparently, in solution.[19]

Conclusions. It is clear from Figure 4 that the absence of a heptacarbonyl or hexacarbonyl stoichiometry for $Cp_2V_2(CO)_n$ is steric in origin. Addition of CO to $Cp_2V_2(CO)_5$ from any perspective appears impossible. Decarbonylation may be accomplished for the similar chromium[20] and molybdenum[21] dimers $Cp_2M_2(CO)_6$ with concomitant reduction in end-to-end nonbonded repulsions. If it is assumed more generally that dimers of the $(hydrocarbon)M(CO)_n$ monomer become unstable for $n \geq 3$, we may also account for the abnormal propensity of $(C_3H_5)_2Fe_2(CO)_6$ to dissociate.[22] The Fe–Fe bond in this dimer has been stretched to exceptional lengths (3.13 Å)[23] in apparent response to the repulsions proposed here.

Although the present study fails in its original intent, the donor semibridge concept may nevertheless be of broad importance in polynuclear metal carbonyl chemistry, particularly for the stabilization of reactive species. Examples include $Cp_2M_2(CO)_4L$ (M = Cr, Mo; L = CO, PR_3), the apparent intermediate in phosphine addition (eq 1) reactions of dimeric

$$Cp_2M_2(CO)_4 + L \rightarrow Cp_2M_2(CO)_4L \xrightarrow{+L} Cp_2M_2(CO)_4L_2 \quad (1)$$

group 6B cyclopentadienyl carbonyls.[21] $Cp_2Mo_2(CO)_5$ has also been detected after flash photolysis of $Cp_2Mo_2(CO)_6$.[24] $Cp_2V_2(CO)_4(PPh_3)$ is thus a close geometric analogue of the intermediate in eq 1. The mechanistic observations of Norton[25] concerning sequential phosphine substitution on $Ir_4(CO)_{12}$ may also be rationalized by using the donor semibridge concept.

The conclusion that V(2) in $Cp_2V_2(CO)_5$ would be an unsaturated-metal center in the absence of electron donation from two carbonyl semibridges is subject to an operational test. To

(16) Drawings of space-filling molecular models were produced by using the program described by: Smith, G. M.; Gund, P. *J. Chem. Inf. Comput. Sci.* **1978**, *18*, 207.

(17) Intermolecular O···H contacts to the ring on V(2) in Ia are longer and less numerous.

(18) Cotton, F. A.; Jamerson, J. D. *J. Am. Chem. Soc.* **1976**, *98*, 1273.
(19) The infrared intensities of Ia or Ib are not significantly altered on changing from hexane solvent to THF.
(20) Hackett, P.; O'Neill, P.; Manning, A. R. *J. Chem. Soc., Dalton Trans.* **1974**, 1625.
(21) Klingler, R. J.; Butler, W.; Curtis, M. D. *J. Am. Chem. Soc.* **1975**, *97*, 3535.
(22) Muetterties, E. L.; Sosinsky, B. A.; Zamaraev, K. I. *J. Am. Chem. Soc.* **1975**, *97*, 5299.
(23) Putnik, C.; Welter, J.; Stucky, G.; D'Aniello, M.; Sosinsky, B.; Kirner, J. F.; Muetterties, E. L. *J. Am. Chem. Soc.* **1978**, *100*, 4107.
(24) Hughey, J. L.; Bock, C. R.; Meyer, T. J. *J. Am. Chem. Soc.* **1975**, *97*, 4440.
(25) Karel, K. J.; Norton, J. R. *J. Am. Chem. Soc.* **1974**, *96*, 6812.

this end, we have studied the mechanism of reactions of $Cp_2V_2(CO)_5$ with donor ligands and we describe these in a separate publication.[26]

Acknowledgment. This research was supported by National Science Foundation Grant No. CHE 77-10059 and by the Marshall H. Wrubel Computer Center.

(26) Lewis, L. N.; Caulton, K. G. *Inorg. Chem.* **1980**, *19*, 1840.

Registry No. Ia, 41699-43-8; Ib, 12185-41-0.

Supplementary Material Available: Listings of observed and calculated structure factors and anisotropic thermal parameters for $Cp_2V_2(CO)_4PPh_3$ and $Cp_2V_2(CO)_5$ and also positional parameters for $Cp_2V_2(CO)_5$ (80 pages). Ordering information is given on any current masthead page.

Contribution from the Department of Chemistry and Molecular Structure Center, Indiana University, Bloomington, Indiana 47405

Hexaisopropoxybis(dimethylamino)dinitrosyldimolybdenum

MALCOLM H. CHISHOLM,* JOHN C. HUFFMAN, and RAYMOND L. KELLY

Received February 5, 1980

Hydrocarbon solutions of $Mo_2(O\text{-}i\text{-}Pr)_6(NO)_2$ react with dimethylamine to form $Mo_2(O\text{-}i\text{-}Pr)_6(HNMe_2)_2(NO)_2$ as a fine microcrystalline precipitate. $Mo_2(O\text{-}i\text{-}Pr)_6(HNMe_2)_2(NO)_2$ shows little solution chemistry: it is only very sparingly soluble in hydrocarbon solvents, and in those which it does dissolve it exists in equilibrium with $Mo_2(O\text{-}i\text{-}Pr)_6(NO)_2$ and free dimethylamine. The compound is also thermally unstable, readily eliminating the coordinated amine with the formation of $Mo_2(O\text{-i-Pr})_6(NO)_2$. The molecular structure has a center of symmetry. Each molybdenum atom is in a distorted octahedral environment, and the halves of the molecule are joined through the agency of a pair of isopropoxy bridges; the Mo-to-Mo distance is 3.390 (2) Å, consistent with the absence of a metal-to-metal bond. There is a linear Mo–N–O moiety (179.4 (5)°) with a short Mo–N distance (1.763 (6) Å). In the infrared spectrum a band at 1617 cm^{-1} is assignable to ν(NO). These results are compared with other recently characterized alkoxynitrosyl compounds of the group 6 transition elements. Crystal data and cell dimensions for $Mo_2(O\text{-}i\text{-}Pr)_6(NO)_2(HNMe_2)_2$ are as follows: space group $P2_1/c$, a = 9.889 (2) Å, b = 11.107 (2) Å, c = 16.901 (3) Å, V = 1576.9 Å^3, β = 121.85 (2)°, Z = 2.

Introduction

Prior work[1-3] has established that the group 6 transition elements form a related series of trialkoxynitrosyl complexes which may take the form of I, II, or III.

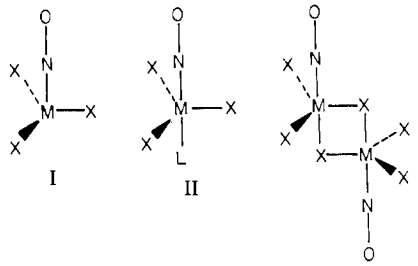

I II III

In I, II, and III there are linear M–N–O groups and the local geometry about the metal atoms contains a trigonal group of alkoxy ligands. Thus when the M–N–O molecular axis is defined as the z axis, there are four electrons in d_{xz} and d_{yz} metal atomic orbitals which are not appreciably used in metal–ligand σ bonding but which are extensively used in metal-to-nitrosyl π^* back-bonding. We report here the preparation and structural characterization of a fourth type of complex in which the metal atom is in a six-coordinate environment as shown in IV.

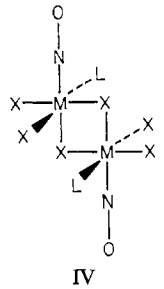

IV

Results

Synthesis and Physicochemical Properties of $Mo_2(O\text{-}i\text{-}Pr)_6(NO)_2(HNMe_2)_2$. Hydrocarbon solutions of $Mo_2(O\text{-}i\text{-}Pr)_6(NO)_2$ react with $HNMe_2$ to yield $Mo_2(O\text{-i-Pr})_6(NO)_2(HNMe_2)_4$ as a microcrystalline red precipitate. The compound is sensitive to moisture and oxygen and must be handled in dry and oxygen-free atmospheres and solvents.

$Mo_2(O\text{-}i\text{-}Pr)_6(NO)_2(HNMe_2)_2$ is thermally unstable: when it is heated in vacuo, dimethylamine is given off and only $Mo_2(O\text{-}i\text{-}Pr)_6(NO)_2$ can be sublimed. In the mass spectrometer the ion of highest mass corresponded to $Mo_2(O\text{-}i\text{-}Pr)_6(NO)_2^+$.

$Mo_2(O\text{-}i\text{-}Pr)_6(NO)_2(HNMe_2)_2$ is only sparingly soluble in hydrocarbon solvents, and ^1H NMR spectra obtained in toluene-d_8 indicate that when it dissolves, it goes into solution to form an equilibrium mixture of $Mo_2(O\text{-}i\text{-}Pr)_6(NO)_2(HNMe_2)_2$, $Mo_2(O\text{-}i\text{-}Pr)_6(NO)_2$, and dimethylamine. ^1H NMR spectra recorded in the presence of excess dimethylamine are consistent with the view that $Mo_2(O\text{-}i\text{-}Pr)_6(NO)_2(HNMe_2)_2$ maintains in solution the structure found in the solid state. Specifically there are three overlapping septets of equal integral intensity in the methyne proton region of the spectrum, as expected for the structure shown in Figure 1 which has three pairs of symmetry related O-i-Pr groups. The methyl groups of each of these O-i-Pr ligands are diastereotopic, and thus six doublets are expected in the isopropoxy methyl region of the spectrum. However, even at 220 MHz we have been unable to separate these: the spectrum simply reveals several overlapping doublets.

Infrared and ^1H NMR data are recorded in the Experimental Section.

Solid-State Structure. In the crystalline state the compound is composed of discrete molecules of $Mo_2(O\text{-}i\text{-}Pr)_6(NO)_2$-

(1) Chisholm, M. H.; Cotton, F. A.; Extine, M. W.; Kelly, R. L. *J. Am. Chem. Soc.* **1978**, *100*, 3354.
(2) Chisholm, M. H.; Cotton, F. A.; Extine, M. W.; Kelly, R. L. *Inorg. Chem.* **1979**, *18*, 116.
(3) Bradley, D. C.; Newing, C. W.; Chisholm, M. H.; Haitko, D. A.; Kelly, R. L.; Little D. A.; Cotton, F. A.; Fanwick, P. E. *Inorg. Chem.*, in press.
(4) Chisholm, M. H.; Cotton, F. A.; Extine, M. W.; Reichert, W. W. *Inorg. Chem.* **1978**, *17*, 2944.

0020-1669/80/1319-2762$01.00/0